

# Geostatistical approach in estimating the capacity volume of the mudflow reservoir

*Khojiakbar Khasanov*<sup>1\*</sup>, *Nodira Babajanova*<sup>1</sup>, *Akylbek Chymyrov*<sup>2</sup> and *Dayanch Reyimov*<sup>3</sup>,  
*Sevar Salokhitdinova*<sup>4</sup>

<sup>1</sup>“Tashkent Institute of Irrigation and Agricultural Mechanization Engineers” National Research University, Tashkent, 100000, Uzbekistan.

<sup>2</sup>Kyrgyz State Technical University named after I. Razzakov, Bishkek, Kyrgyzstan

<sup>3</sup>International horse breeding academy named after Aba Annaev, Arkadag city, Turkmenistan

<sup>4</sup>National University of Uzbekistan named after Mirzo Ulugbek, Tashkent, Uzbekistan

**Abstract.** Mudflow reservoirs play a crucial role in mitigating flood risks triggered by natural events like heavy rains and snowmelt, safeguarding surrounding areas from potential inundation. However, sedimentation poses a significant challenge by reducing the capacity and effectiveness of these mudflow reservoirs over time. This study focused on estimating the capacity of the Kalkama mudflow reservoir, constructed in 1987, using a geostatistical approach. Bathymetric survey data were analyzed using various interpolation methods. Kriging (Ordinary Kriging) provided the best performance with the lowest RMSE (0.28) and a high  $R^2$  (0.99), indicating it is the most accurate method for this dataset. Based on this method, a spatial model of the mudflow reservoir was developed to assess its current capacity. Findings indicate a capacity loss of 2.33 million  $m^3$  (23.6%) over 36 years, alongside a 22% reduction in surface area at Full Storage Level, and the dead volume was completely filled with sediment.

## 1 Introduction

Mudflow reservoirs play a crucial role in managing and regulating mudflows triggered by heavy rains, snow melting, or other natural processes, aiming to prevent floods and safeguard surrounding areas and populations [1,2]. These reservoirs are strategically designed to capture and retain significant volumes of water, thereby mitigating the impact of mudflows and reducing the associated risks [3]. It can be understood from several studies that utilizing existing reservoirs for flood water retention is a crucial strategy in flood risk management, necessitating comprehensive plans integrating reservoir operation adjustments based on detailed studies and analyses [4–6]. Research emphasizes the importance of assessing reservoir performance under flood conditions, introducing innovative approaches like the standard operation policy and ideal approach to enhance flood mitigation through optimized reservoir operations [4]. Furthermore, the concept of resilience is introduced to measure the ability of flood control systems to recover after extreme floods, highlighting the need for reservoirs to not only reduce flood risks but also to bounce back to their original states

---

\* Corresponding author: [kh.khasanov@outlook.com](mailto:kh.khasanov@outlook.com)

efficiently [7]. By considering factors like upstream reservoir management, anthropogenic activities, and the balance between conflicting demands during uncertain inflows, reservoir operation adjustments can play a pivotal role in effective flood risk management [6,8].

Mudflow reservoirs in Uzbekistan are predominantly found in mountainous and foothill areas, with the most mudflow-prone regions being Namangan, Fergana, Surkhandarya, Tashkent, Kashkadarya, and Samarkand, with the Fergana Valley alone accounting for 41% of all registered mudflows [9]. Climate change is expected to exacerbate mudflow occurrences in piedmont areas of Uzbekistan, with projections indicating an increase in mudflow-generating weather patterns by up to 5% by the end of the century [10]. Climate change adaptation strategies are crucial to mitigate the projected increase in flood activity in Uzbekistan. Studies emphasize the importance of implementing various measures, such as systems reoperation in water management [11], enhancing retention reservoirs, and river dike construction [12]. Additionally, the development of hybrid solutions combining green and grey infrastructure is highlighted as effective in flood risk management, especially in Central-Eastern European countries like Uzbekistan [13]. The potential risks posed by glacial lakes outburst floods in Central Asia due to climate change are acknowledged, emphasizing the need for accurate digital elevation models and flood parameters for effective flood prevention and reservoir operation [14].

Sedimentation presents a substantial challenge for mudflow reservoirs, impacting their storage capacity and operational sustainability [15,16]. Globally, reservoirs are losing storage capacity due to sedimentation, with estimates indicating a 26% storage loss by 2050, affecting regions like Asia-Pacific and Africa differently [17]. Sedimentation poses a significant challenge for mudflow reservoirs in Uzbekistan, impacting their functionality and water storage capacity [18–20]. The high sedimentation rates in the major rivers of Central Asia, such as Amu Darya and Syr Darya, result in the accumulation of turbid sediments in these reservoirs, reducing their volume capacity and affecting water availability for irrigation and other purposes [21,22].

Accurate knowledge of storage capacity is indeed crucial for implementing effective climate change adaptation strategies and utilizing mudflow reservoirs globally. Studies emphasize the significance of reservoir operational reliability assessment under current and future climate conditions, highlighting the importance of understanding storage capacity to ensure water availability [23]. Furthermore, the review on climate change adaptation strategies in water management stresses the need for updating reservoir operation curves and optimizing reservoir storage to enhance resilience to climate change impacts [11].

Determining the current capacity of a water reservoir involves a variety of methods tailored to data availability, reservoir type, and required precision. Determining the current capacity of a water reservoir involves a variety of tailored methods, including bathymetric surveys, GIS, remote sensing, hydrological modeling, manual measurements, capacity tables, and geostatistical analysis. For example, a method for measuring water surface area and storage volume using multi-sensor satellite remote sensing data through the Tuyen Quang Reservoir case study in Northern Vietnam is proposed [24]. Hydrological models and capacity tables are employed for the Three Gorges Reservoir in China [25]. Engineers at the Aswan High Dam in Egypt conduct manual measurements and use capacity curves alongside satellite imagery [26,27]. Geostatistical analysis and bathymetric surveys are applied to Lake Kariba in Zambia-Zimbabwe [28]. The Sardar Sarovar Dam reservoir in India utilizes capacity tables and remote sensing for efficient water resource management [29]. These methods offer a comprehensive assessment guiding reservoir management and maintenance decisions.

The objective of this study is to evaluate the storage capacity of the Kalkama mudflow reservoir, constructed in 1987 in Uzbekistan, through the application of a geostatistical methodology. To achieve this, bathymetric survey data collected in 2023 were used. The data

were processed and interpreted using a variety of interpolation techniques to develop an accurate spatial model, providing insights into the reservoir's current state and sedimentation levels.

## 2 Materials and Methods

### 2.1 Study area

The Kalkama mudflow reservoir is located in the Chirakchi District of Kashkadarya Province, approximately 40 km northwest of the district center. It was constructed in the Kumdarya riverbed and has been in operation since 1987. The reservoir is designed to manage floodwaters and provide water for agricultural purposes.

**Table 1.** Main indicators for mudflow reservoir.

Indicator	Value
Full storage capacity	9.45 M m <sup>3</sup>
Active storage capacity	9.35 Mm <sup>3</sup>
Dead storage capacity	0.1 Mm <sup>3</sup>
Maximum storage level (MFL)	679.0 m.a.s.l
Full storage level (FSL)	677.2 m.a.s.l
Dead storage level (DSL)	663.0 m.a.s.l
Dam Crest Elevation	680.0 m.a.s.l
Surface Area at FSL	15 km <sup>2</sup>
Surface Area at DSL	0.11 km <sup>2</sup>
<b>Earthen Dam</b>	
- Maximum Height	21 m
- Crest Length	546 m
- Crest Width	10 m

In the winter-spring months, little precipitation is observed. Average annual precipitation is 250–295 mm. Precipitation is observed mainly in November-April. The period of most precipitation falls on March-April. The summer season is dry and there is almost no precipitation for 3-4 months. Average annual evaporation is 1300 mm.

### 2.2 Bathymetric measurements

Bathymetric measurements are important for understanding the ecosystem of bodies of water, especially rivers, lakes, and reservoirs. It is essentially vital to various hydrological and ecological processes. Accurate bathymetric surveys, whether through traditional methods like lead lines and echosounders [30] or modern techniques like satellite bathymetry and sonars [31], provide valuable insights into the topography of underwater terrains. This data aids in predicting climate change effects on water supply, measuring flood hazards, and enhancing hydrological models [32]. Furthermore, detailed bathymetric representation influences surface water-groundwater interactions, infiltration rates, and overall hydrodynamic routing in river networks, showcasing the interconnectedness of surface and subsurface processes [33,34].

Bathymetric measurements can be conducted using various techniques, including traditional and innovative methods. Traditional methods involve using SingleBeam and Multibeam EchoSounders (SBES and MBES) [35,36], which provide depth data for mapping underwater topography. Innovative approaches include LiDAR, Satellite Derived Bathymetry (SDB), Synthetic Aperture Radar (SAR) techniques for airborne or spaceborne

measurements [37,38]. Additionally, in situ techniques like Unmanned Autonomous Vehicles (UAVs), Underwater Drones, Remotely Operated Vehicles (ROVs), and Autonomous Survey Vessels (ASVs/USVs) are increasingly utilized for bathymetric surveys, especially in shallow coastal areas and offshore environments [39–41].

Bathymetric surveys were carried out in April 2023 at the Kalkama mudflow reservoir to determine the level of siltation. During this period, there were favorable weather conditions at the reservoir, which ensured good visibility and accuracy of the survey. The surveys were conducted using the APACHE 3 (Figure 1) single-beam echo sounder, specifically designed for bathymetric surveys of lakes, reservoirs, inland rivers, and coastal areas. The USV moved along the water surface of the Kalkama mudflow reservoir along predetermined cross sections using GPS equipment GNSS i90. The cross-sections (27 in total) of the water surface of the reservoir were divided every 100 meters according to the technical specifications. Vertical depth measurements were carried out at intervals of up to 1 meters (Figure 2).

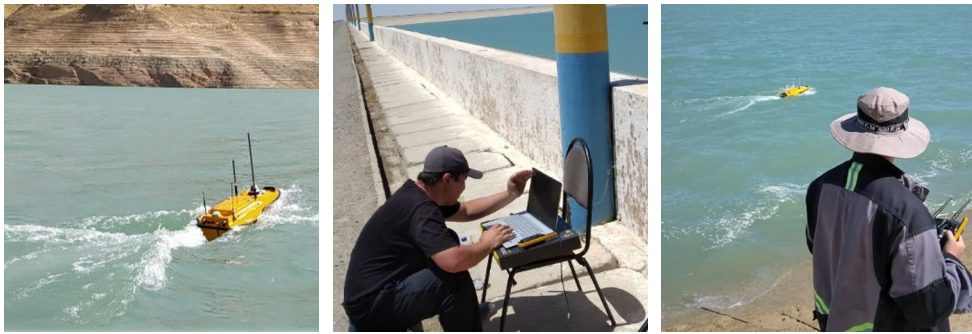


**Fig. 1.** Bathymetric survey process

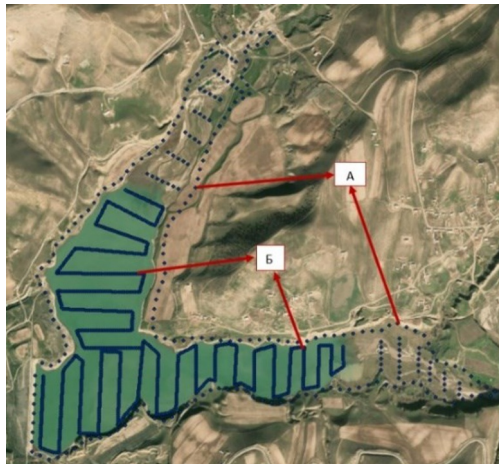


**Fig. 2.** The distribution of topometric (A) and bathymetric (B) surveys

The use of advanced equipment and software enabled the collection of precise and comprehensive data on the underwater topography and sedimentation levels of the reservoir. This information is critical for the effective management and maintenance of the reservoir's capacity and functionality.

### 2.3 Data processing

Bathymetric data processing plays a crucial role in creating accurate digital terrain models for reservoir sedimentation management, and coastal studies [42,43]. Interpolation

(deterministic and geostatistical) techniques are commonly used for generating high-quality Digital Elevation Models (DEMs) of the seafloor or reservoir bottoms [44]. The quality of depth data is essential for various applications, and the use of deterministic and geostatistical techniques can significantly impact the accuracy of the bathymetric data [42]. The distance between points taken in bathymetric measurements plays a significant role when choosing interpolation techniques, both deterministic and geostatistical. In this process, the distance between points obtained in bathymetric measurements is important in choosing interpolation methods.

Given the specific configuration of your data points—where the horizontal distance between cross-sections is 100 meters and the vertical distance between points within each cross-section is 1 meters—this survey has a linear arrangement of data points in a grid-like pattern.

Deterministic interpolation techniques like Inverse Distance Weighting (IDW), spline interpolation, and Radial Basis Function (RBF) interpolation each have their strengths and limitations when applied to spatial data with large horizontal gaps. IDW may oversmooth data when points are uniformly distributed, impacting accuracy [45]. Spline interpolation can create a smooth surface but might not effectively handle large horizontal gaps, focusing more on overall trends than local variations [46]. On the other hand, RBF interpolation fits a smooth surface through data points using radial basis functions, but it may not be optimal for datasets with significant horizontal gaps [47].

Kriging is a powerful geostatistical technique that can effectively capture spatial correlation structures in both horizontal and vertical directions, making it suitable for handling anisotropy by adjusting the variogram [48,49]. Co-Kriging, on the other hand, leverages secondary information to enhance interpolation accuracy, but it is more complex and requires additional correlated data, making it less relevant without such supplementary datasets [50]. Empirical Bayesian Kriging (EBK) emerges as a robust method for interpolating bathymetric data, especially in scenarios with high variability and uncertainty, offering automated variogram modeling and uncertainty quantification for structured cross-section measurements. Despite its computational intensity due to multiple variogram fitting processes, EBK is recommended for precise and reliable results, although it may be more complex to grasp compared to simpler deterministic methods like IDW or spline [43].

## **3 Result and discussion**

### **3.1 Result of geostatistical work**

The geostatistical analysis for the bathymetric data of the Kalkama mudflow reservoir was carried out using different interpolation methods. Interpretation of results Root Mean Squared Error (RMSE) [51] and Coefficient of Determination ( $R^2$ ) [52] results were taken into account. Measures the average magnitude of the errors between predicted and observed values. Lower RMSE indicates a more accurate model and indicates the proportion of the variance in the observed data that is predictable from the model, values closer to 1 suggest a better fit.

The results of the analysis: Kriging (Ordinary Kriging) provided the best performance with the lowest RMSE (0.28) and a high  $R^2$  (0.99), indicating it is the most accurate method for this dataset. EBK also showed good performance with a low RMSE (0.34) and a high  $R^2$  (0.99), making it a reliable alternative. RBF had a moderate performance with an RMSE of 0.40 and an  $R^2$  of 0.97, which is less accurate than Kriging and EBK. IDW had the highest RMSE (0.79), suggesting it is the least accurate method among those tested, despite having a high  $R^2$  (0.99).

For the bathymetric analysis of the Kalkama mudflow reservoir, Ordinary Kriging is the recommended interpolation method due to its superior accuracy and reliability. EBK is a strong alternative, especially beneficial for complex data handling. RBF, while less accurate, can be considered if computational resources are limited. IDW is the least preferred method for this application due to its higher error rate.

After conducting the geostatistical analysis and selecting the optimal interpolation method (Ordinary Kriging), the resulting spatial model of the Kalkama mudflow reservoir was processed (Figure 3).

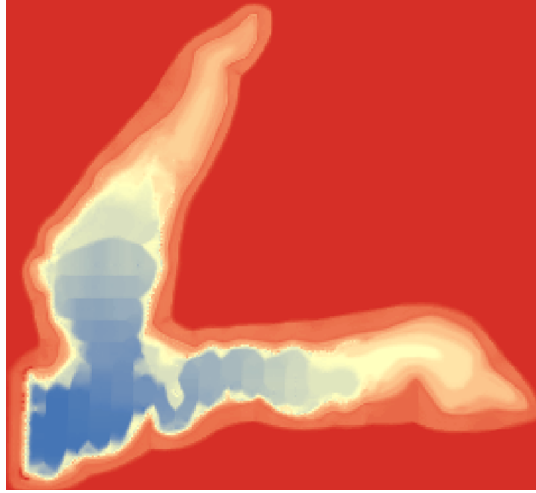


**Fig. 3.** Spatial model of mudflow reservoir (Ordinary Kriging)

The spatial model derived from the Ordinary Kriging interpolation method was exported to a raster format. This format is suitable for digital representation and analysis of geographic data. The raster model had cut along the surface of the MFL (679.0 m.a.s.l) mark. The MFL mark indicates the maximum operational water level of the reservoir. A bathymetric map is developed from special data (Figure 4). The exported raster format represents a digital elevation model (DEM) of the mudflow reservoir bowl. The DEM captures the underwater topography and sedimentation levels of the reservoir, providing a detailed 3D representation of the reservoir's bottom surface (Figure 5).

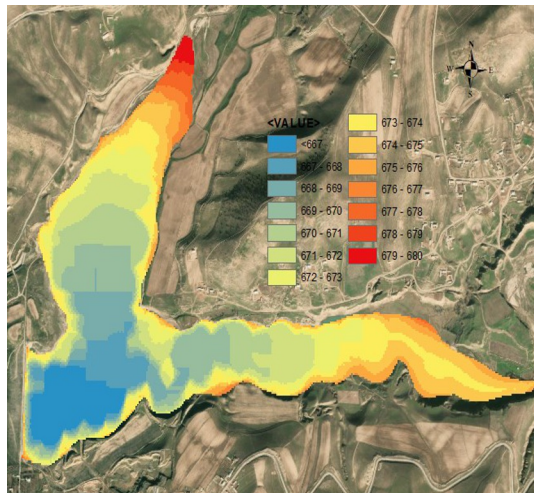


**Fig. 4.** Bathymetric map of the mudflow reservoir bowl

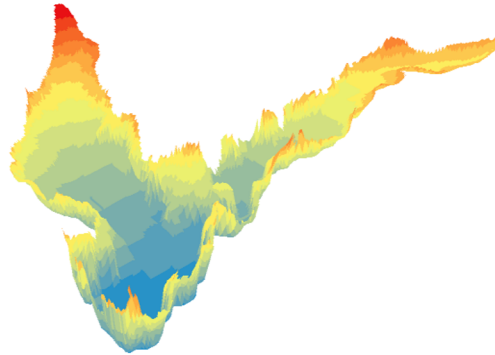


**Fig. 5.** 3D model of the mudflow reservoir bowl

### 3.2 Results of calculation capacity volume of mudflow reservoir

The tool described is designed for computing storage area capacities and storage volumes using an input surface raster and a series of specified stage heights (levels). Known as the "Function Storage Volume" tool, it performs calculations to determine the storage area capacities and storage volumes for various stage heights within a given input surface raster. This functionality is critical for understanding the volume and area of water that can be stored at different levels in a reservoir or similar structure.

The parameters for calculating the capacity of the Kalkama mudflow reservoir include a maximum height of 677.3 meters above sea level (masl), a minimum height of 666.0 masl, and an incremental value of 0.1 meters for stage height increments.

The results are presented in detailed tabular form and graphs showing the total storage area and storage volume size corresponding to each stage height in the specified range. The general conclusion is given in the form of a report. The results can be copied to Excel or similar programs for other purposes. The data obtained for the Kalkama mudflow reservoir is presented in Table 3 (Table 3). The generated curves (volume-elevation) from this study are shown.

**Table 2.** The volume coordinates of the Kalkama mudflow reservoir storage (Mm<sup>3</sup>).

Elevation (m)	0.00	0.1	0.20	0.3	0.40	0.5	0.60	0.7	0.80	0.9
666.0						0.01	0.01	0.02	0.03	0.04
667.0	0.05	0.06	0.07	0.08	0.09	0.10	0.11	0.13	0.14	0.16
668.0	0.17	0.19	0.21	0.23	0.24	0.27	0.29	0.31	0.33	0.36
669.0	0.38	0.41	0.43	0.46	0.49	0.52	0.56	0.59	0.62	0.66
670.0	0.70	0.73	0.77	0.82	0.86	0.90	0.95	1.00	1.05	1.10
671.0	1.15	1.20	1.25	1.30	1.36	1.41	1.47	1.53	1.59	1.65
672.0	1.71	1.78	1.85	1.92	2.00	2.07	2.14	2.22	2.30	2.37
673.0	2.45	2.53	2.62	2.70	2.79	2.88	2.96	3.05	3.14	3.23
674.0	3.32	3.42	3.51	3.61	3.71	3.81	3.91	4.01	4.12	4.22
675.0	4.33	4.44	4.56	4.67	4.79	4.91	5.03	5.15	5.28	5.40
676.0	5.53	5.67	5.80	5.94	6.08	6.22	6.36	6.50	6.64	6.79
677.0	6.93	7.07	7.22							

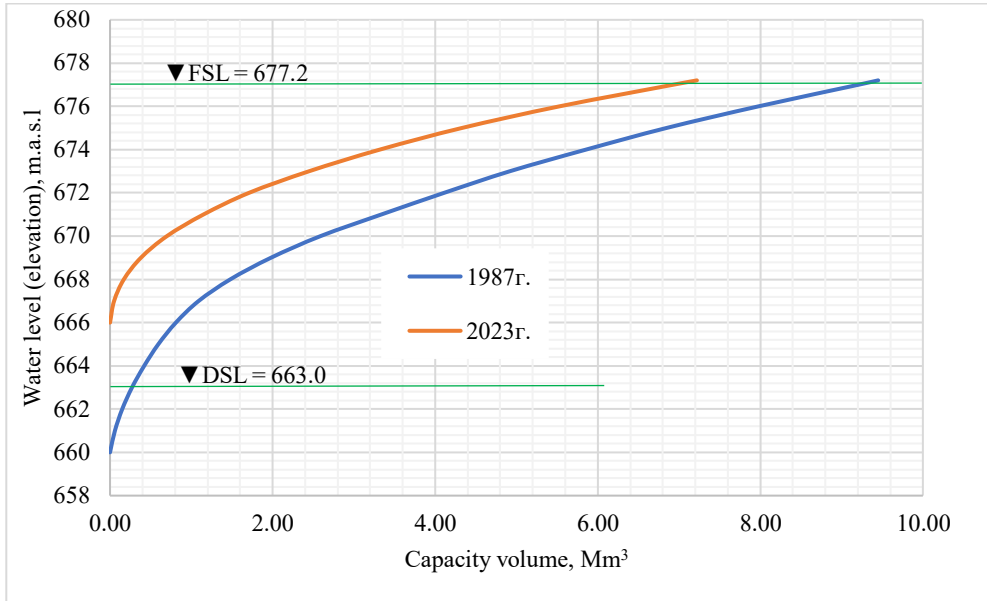


**Fig. 1.** Caption of the Figure 1. Below the figure.

The research results indicate that over 36 years of operation, the landslide reservoir lost 2.33 Mm<sup>3</sup> of capacity, which represents a reduction of 23.6% in volume. The reservoir's surface area decreased from 1.0 km<sup>2</sup> to 0.78 km<sup>2</sup> at the maximum water level, a reduction of 22%. The dead volume was completely filled with sedimentation (Figure 6).

## 4 Conclusions

When floods or floodwaters enter the mudflow reservoir, significant amounts of silt and sediment are deposited, altering the reservoir's volume. Knowing the exact size of the mudflow reservoir is crucial for its safe and effective operation. In this research, various interpolation methods were analyzed to process bathymetric measurement results obtained using modern tools, with the goal of determining the size of the Kalkama flood reservoir and developing a spatial model. Among the methods analyzed, simple Kriging proved effective in creating an accurate spatial model from bathymetric data.

Based on the spatial model, the volume loss of the flood reservoir over 36 years of operation was analyzed. The results showed a capacity reduction of 2.33 million m<sup>3</sup>, representing a 23.6% decrease in volume. Additionally, the surface area of the mudflow reservoir at the FSL decreased from 1.0 km<sup>2</sup> to 0.78 km<sup>2</sup>, a reduction of 22%. The dead volume of the reservoir was completely filled with sedimentation.

Sedimentation in reservoirs is a natural process that diminishes their water storage capacity, but various measures can mitigate its effects. For example, afforestation, bank reinforcement, sediment-trapping structures, hydraulic flushing, mechanical dredging, installing sediment removal devices, operating spillways, flushing gates, releasing turbid water through tunnels, and raising intake structure levels or dam height to manage sediment effectively and other.

## Acknowledgements

LLC "Center for Safety Assessment and Monitoring of Hydrotechnical Facilities" generously contributed bathymetric data. The authors would like to express their gratitude to all members of the hydrographic survey crew who assisted them with this effort. Furthermore, they appreciate the employees of the operation of the Kalkama mudflow reservoir for providing historical bathymetric and other data.

## References

1. A. Adzhiev, N. Kondratyeva, and A. Kortiev, Sustainable Development of Mountain Territories **15**, 984 (2023)
2. B. Zh. Imamova and A. K. Murzalimova, Bulletin of Shakarim University. Technical Sciences **1**, 53 (2023)
3. A. Yangiev, D. Adjimuradov, S. Panjiev, and R. Karshiev, E3S Web of Conferences **264**, 03033 (2021)
4. M. Zarei, O. Bozorg-Haddad, and H. A. Loáiciga, J Hydrol (Amst) **624**, 129774 (2023)
5. M. Połomski and M. Wiatkowski, Sustainability **15**, 16020 (2023)
6. N. J. Shanono, M. L. Attanda, N. M. Nasidi, M. D. , Zakari, A. Ibrahim, M. N. Yahya, I. M. T. Usman, A. H. Abdullahi, and S. I. Umar, FUDMA JOURNAL OF SCIENCES **7**, 125 (2023)
7. W. Ding, G. Wei, and H. Zhou, J Hydrol (Amst) **620**, 129494 (2023)
8. S. K. Jain, L. S. Shilpa, D. Rani, and K. P. Sudheer, J Hydrol (Amst) **618**, 129165 (2023)
9. I. Dergacheva, S. Klimov, G. Khamdamova, Q. Raximov, and T. Apakhujayeva, E3S Web of Conferences **263**, 02019 (2021)
10. G. Mamadjanova and G. C. Leckebusch, Weather Clim Extrem **35**, 100403 (2022)
11. M. Elgandy, S. Hassini, and P. Coulibaly, J Hydrol Eng **29**, (2024)
12. H. W. Jee, S. B. Seo, K. Ko, J. Cho, and Y. Chae, J Flood Risk Manag **17**, (2024)
13. N. Bezak, M. Šraj, P. Raška, L. Slavikova, and J. Jakubínský, in *EGU General Assembly* (Vienna, 2023)
14. G. Umirzakov, E. Semakova, D. Junsaliev, T. Sabitov, H. Mamirov, and A. Cicoira, in *EGU23, the 25th EGU General Assembly* (Vienna, 2023), p. EGU-13286
15. C. Wenhong, River **1**, 121 (2022)
16. Y. K. Saito, L. J. F. Viana, Í. O. Ferreira, and E. A. G. Marques, Earth Sciences Research Journal **25**, 193 (2021)
17. D. Perera, S. Williams, and V. Smakhtin, Sustainability **15**, 219 (2022)
18. M. Bakiev and K. Khasanov, International Journal of Geoinformatics **17**, 37 (2021)
19. K. Khasanov, IOP Conf Ser Mater Sci Eng **883**, (2020)
20. Bakiev, M. Khasanov, K. and Primbetov, I., International Journal of Geoinformatics **53** (2022)
21. S. Rakhmatullaev, F. Huneau, H. Celle-Jeanton, P. Le Coustumer, M. Motelica-Heino, and M. Bakiev, Environ Earth Sci **68**, 985 (2013)
22. S. Rakhmatullaev, F. Huneau, M. Bakiev, M. Motelica-Heino, and P. Le Coustumer, in *IAHS-AISH Publication* (2011), pp. 171–181
23. H. M. L. Chaves, C. C. da Silva, and M. R. S. Fonseca, Water (Basel) **15**, 2323 (2023)
24. T. Nguyen Thien Phuong, T. Nguyen Duy, H. Nguyen Thi Thu, V. Pham Quang, and T. Dinh Xuan, Vietnam Journal of Earth Sciences (2023)
25. V. Lakshmi, J. Fayne, and J. Bolten, J Hydrol (Amst) **567**, 510 (2018)

26. C. S. Reddy, K. R. L. Saranya, C. S. Jha, V. K. Dadhwal, and Y. V. N. K. Murthy, *Remote Sens Appl* **8**, 114 (2017)
27. El-Fadel M., Zeinati M., and Jamali D., *Environ Manage* **55**, 892 (2015)
28. S. Wang, Y. Cui, A. Li, W. Zhang, D. Wang, Z. Chen, and J. Liang, *J Environ Manage* **260**, 110159 (2020)
29. Patel P.L., Singh R.K., and Sharma J., *Int J Remote Sens* **40**, 8798 (2019)
30. K. T. Martinsen, K. Sand-Jensen, and R. Selvan, *Limnol Oceanogr Methods* **21**, 625 (2023)
31. M. Wróbel, K. Mańk, R. Gawryś, A. K. Kaniewska, A. Boczoń, and S. Grajewski, *International Journal of Hydrology Science and Technology* **16**, 82 (2023)
32. A. I. Pathan, D. Patel, D. R. Samal, C. Prieto, and S. Eslamian, in *Handbook of Hydroinformatics* (Elsevier, 2023), pp. 339–351
33. B. Khazaei, L. K. Read, M. Casali, K. M. Sampson, and D. N. Yates, *Sci Data* **9**, 36 (2022)
34. S. Dey, S. Saksena, D. Winter, V. Merwade, and S. McMillan, *Water Resour Res* **58**, (2022)
35. Khomsin, D. G. Pratomo, and I. Saputro, *IOP Conf Ser Mater Sci Eng* **1052**, 012015 (2021)
36. A. Makar, *Sensors* **23**, 4215 (2023)
37. A. Szafarczyk and C. Toś, *Sensors* **23**, 292 (2022)
38. M. I. Prasetya, V. P. Siregar, and S. B. Agus, *Jurnal Kelautan Tropis* **26**, 113 (2023)
39. O. Lewicka, M. Specht, A. Stateczny, C. Specht, G. Dardanelli, D. Brčić, B. Szostak, A. Halicki, M. Stateczny, and S. Widźgowski, *Remote Sens (Basel)* **14**, 4075 (2022)
40. J. Fan, H. Pei, and Z. Lian, *J Mar Sci Eng* **11**, 770 (2023)
41. L. Apicella, M. De Martino, I. Ferrando, A. Quarati, and B. Federici, *J Mar Sci Eng* **11**, 671 (2023)
42. Z. Li, Z. Peng, Z. Zhang, Y. Chu, C. Xu, S. Yao, Á. F. García-Fernández, X. Zhu, Y. Yue, A. Levers, J. Zhang, and J. Ma, *Front Mar Sci* **10**, (2023)
43. W. Mujta, M. Włodarczyk-Sielicka, and A. Stateczny, *Sensors* **23**, 5445 (2023)
44. D. G. Pratomo, R. A. D. Safira, and O. Stefani, *Geodesy and Cartography* **49**, 186 (2023)
45. P. A. Verma, H. Shankar, and S. Saran, in *Remote Sensing of Northwest Himalayan Ecosystems* (Springer Singapore, Singapore, 2019), pp. 537–547
46. I. V. Yuyukin, *Vestnik Gosudarstvennogo Universiteta Morskogo i Rechnogo Flota Imeni Admirala S. O. Makarova* **14**, 875 (2022)
47. P. Biernacik, W. Kazimierski, and M. Włodarczyk-Sielicka, *Sensors* **23**, 3941 (2023)
48. J. Angel, J. Behrens, S. Götschel, M. Hollm, D. Ruprecht, and R. Seifried, *Comput Fluids* **278**, 106321 (2024)
49. N. Khakhim, A. Kurniawan, P. Wicaksono, and A. Hasrul, *Journal of Environmental Management and Tourism* **15**, 41 (2024)
50. Z. Hao, F. Chen, X. Jia, X. Cai, C. Yang, Y. Du, and F. Ling, *Water Resour Res* **60**, (2024)
51. A. M. Reed, in (2023), pp. 291–303
52. G. P. Adhikari, *Scholars' Journal* **22** (2022)